SLAC–PUB–5159
February 23, 1990
T/E

OBSERVATION OF A PSEUDOSCALAR STATE IN $J/\psi \to \gamma\phi\phi$ NEAR $\phi\phi$ THRESHOLD*

Z. Bai, G.T. Blaylock, T. Bolton, T.E. Browder, J.S. Brown, K.O. Bunnell, T.H. Burnett, R.E. Cassell, D. Coffman, V. Cook, F. DeJongh, D.E. Dorfan, J. Drinkard, G.P. Dubois, G. Eigen, K.F. Einsweiler, B.I. Eisenstein, T. Freese, C. Gatto, G. Gladding, J. Hauser, C.A. Heusch, D.G. Hitlin, J.M. Izen, P.C. Kim, J. Labs, A. Li, W.S. Lockman, U. Mallik, C.G. Matthews, A.I. Mincer, R. Mir, P.M. Mockett, R.F. Mozley, B. Nemati, A. Odian, L. Parrish, R. Partridge, D. Pitman, S.A. Plaetzer, J.D. Richman, H.F.W. Sadrozinski, M. Scarlatella, T.L. Schalk, R.H. Schindler, A. Seiden, C. Simopoulos, I.E. Stockdale, W. Toki, B. Tripsas, F. Villa, M.Z. Wang, S. Wasserbaech, A.J. Weinstein, S. Weseler, H.J. Willutzki, D. Wisinski, W.J. Wisniewski, R. Xu, Y. Zhu

The Mark III Collaboration

California Institute of Technology, Pasadena, CA 91125
University of California at Santa Cruz, Santa Cruz, CA 95064
University of Illinois at Urbana-Champaign, Urbana, IL 61801
University of Iowa, Iowa City, IA 52242
Stanford Linear Accelerator Center, Stanford, CA 94309
University of Washington, Seattle, WA 98195

Abstract

We present a study of the radiative decay $J/\psi \to \gamma\phi\phi$ in the $\gamma K^+K^-K^+K^-$ and $\gamma K^+K^-K^0_SK^0_L$ final states. A pseudoscalar state is observed in the $\phi\phi$ invariant mass spectrum at 2.22 GeV/c^2 with a width of 150 MeV/c^2. The product branching ratios are $B(J/\psi \to \gamma X) \cdot B(X \to \phi\phi) = (3.3 \pm 0.8 \pm 0.5) \times 10^{-4}$ for the $\gamma K^+K^-K^+K^-$ mode and $B(J/\psi \to \gamma X) \cdot B(X \to \phi\phi) = (2.7 \pm 0.6 \pm 0.6) \times 10^{-4}$ for the $\gamma K^+K^-K^0_SK^0_L$ mode. No evidence for 2^{++} states below 2.4 GeV/c^2 is found in this radiative J/ψ decay mode.

Submitted to *Physical Review Letters*

* This work was supported in part by the U.S. Department of Energy, under contracts DE-AC03-76SF00515, DE-AC02-76ER01195, DE-AC02-87ER40318, DE-AC03-81ER40050, DE-AM03-76SF0034, and by the National Science Foundation.

Interest has focused recently on the $\phi\phi$ system produced in radiative J/ψ decays, since this process may produce glueballs, hybrids or four quark states.[1] Structures in the $\phi\phi$ invariant mass spectrum have been observed by several experiments in the reaction $\pi^- p \rightarrow \phi\phi n$.[2] One group, after performing a partial wave analysis, has resolved three broad 2^{++} resonances near $\phi\phi$ threshold. These states have been claimed to be glueballs,[3] since the production process is Okubo-Iizuka-Zweig (OZI) suppressed. If this hypothesis is correct, these states should also be produced in radiative J/ψ decays[1]. The DM2 group[4] has reported the observation of a low-mass enhancement in $J/\psi \rightarrow \gamma\phi\phi$ at 2.25 GeV/c^2 with a preferred spin-parity of $J^P = 0^-$. Other pseudoscalar states near threshold as well as at higher mass have been observed [5] in radiative J/ψ decays to $\rho\rho$ and $\omega\omega$; the $\eta(2100)$ is the only state kinematically accessible to $\gamma\phi\phi$. We present herein a study of $J/\psi \rightarrow \gamma\phi\phi$ in the $\gamma K^+K^-K^+K^-$ and $\gamma K^+K^-K^0_S K^0_L$ final states[6], using 4.9×10^6 produced J/ψ events recorded with the Mark III detector[7] at the SLAC e^+e^- storage ring SPEAR.

The study of the $\gamma K^+K^-K^+K^-$ channel is made difficult by kaon decays which severely affect the detection efficiency, especially at low $\phi\phi$ masses ($m_{\phi\phi}$), where kaon momenta are smallest. For $m_{\phi\phi}$ below 2.4 GeV/c^2, 60% of all events with four observed charged tracks suffer from momentum mismeasurements because of track kinks due to decays in flight. A four constraint (4C) kinematic fit to the hypothesis $J/\psi \rightarrow \gamma K^+K^-K^+K^-$ typically fails for these events. A substantial increase in detection efficiency can be obtained with 1C kinematic fits to the hypothesis $J/\psi \rightarrow \gamma K^+K^-K^\pm(K^\mp_{miss})$, where the most poorly-measured track is excluded from the fit. To ensure a consistent procedure for events with four well-measured tracks, a 1C fit is performed to all three-track combinations by omitting one track at a time, retaining the fit with the lowest χ^2. In events with several isolated photon candidates[8], the radiative photon is always chosen to be the shower closest to the direction of the missing momentum of the four charged tracks. Candidates are selected from events which have: at least two well-identified kaon tracks[9], no pion candidate [9] (unless two like-sign kaons are found), a 1C fit probability greater than 2%, and less than five isolated photons.

Figure 1a shows a scatter plot of the invariant masses $m_{K^+K^-}$ versus $m_{K^\pm K^\mp_{miss}}$. A clear $\phi\phi$ signal is observed, providing evidence for the process $J/\psi \to \gamma\phi\phi$, since the modes $J/\psi \to \phi\phi$ and $J/\psi \to \phi\phi\pi^0$, are forbidden by C-invariance. The final $\phi\phi$ sample is extracted by requiring $|m_{K\bar{K}} - m_\phi| \leq 3\sigma$, where the measured resolutions are $\sigma_{K^+K^-} = 3.8$ MeV/c^2 and $\sigma_{K\bar{K}_{miss}} = 5.9$ MeV/c^2. The resulting $\phi\phi$ invariant mass spectrum for the 1C fit events, shown in Figure 2a, contains a total of 168 events. The mass resolution, determined by Monte Carlo simulation, varies from 12 MeV/c^2 at 2.2 GeV/c^2 to 19 MeV/c^2 in the η_c region. Potential background sources consist of modes such as $\gamma\phi K^+K^-$, ϕK^+K^-, $\phi K^+K^-\pi^0$, and $K^+K^-\ \pi^+\pi^- + n\gamma$. The background is estimated from the events inside the lightly-shaded areas in Figure 1a, after subtracting the contribution from the darkly-shaded areas and correcting for feedthrough from real $\gamma\phi\phi$ events as determined from a Monte Carlo simulation. The background, amounting to 9%, is uniform in $m_{\phi\phi}$.

Figure 2c shows the $\phi\phi$ invariant mass spectrum after efficiency correction. A prominent structure around 2.2 GeV/c^2 is visible, as is the η_c. The mass spectrum is fitted to a relativistic p-wave Breit-Wigner line shape with a mass dependent width [10] but without a form factor, a non-relativistic Breit-Wigner line shape for the η_c, a uniform background and three-body phase-space. Table I summarizes the results. For the low mass state,[11] the mass, width and product branching ratio are $M = 2230 \pm 25 \pm 15$ MeV/c^2 and $\Gamma = 150^{+300}_{-60} \pm 60$ MeV/c^2 and $B(J/\psi \to \gamma X) \cdot B(X \to \phi\phi) = (3.3 \pm 0.8 \pm 0.5) \times 10^{-4}$. The systematic errors includes uncertainties in the luminosity measurement, event selection, background subtraction, efficiency determination and fit. We have also made fits which include a production and decay form factor using both Blatt-Weisskopf and Gaussian shapes. A dispersion relation was used [12], to ensure a proper form-factor cutoff at infinity. Within errors, the mass and width remain the same, but the branching ratio increases by up to a factor of two, as the fit attempts to accommodate the cluster of events around 2.5 GeV. This is not, however, a realistic description, since the events around 2.5 GeV are not $J^P = 0^-$ (*see below*). For the η_c, the mass and width are found to be in good agreement with nominal values;[13] the product branching ratio is consistent with the previous Mark III result, which was based on the first half of the data sample.[14] The total branching ratio for radiative $\phi\phi$ production is $B(J/\psi \to \gamma\phi\phi) = (7.5 \pm 0.6 \pm 1.2) \times 10^{-4}$.

There are 80 events which have satisfactory 4C kinematic fits to the $\gamma K^+K^-K^+K^-$ hypothesis. Due to the small detection efficiency at low $m_{\phi\phi}$ the η_c is the only significant signal observed in the $\phi\phi$ mass spectrum. The events in the low mass region, however, are consistent with the signal events in the 1C fit. The η_c mass so obtained, $2969 \pm 4 \pm 4$ MeV/c^2, and product branching ratio, $B(J/\psi \to \gamma\eta_c) \cdot B(\eta_c \to \phi\phi) = (0.94 \pm 0.23 \pm 0.16) \times 10^{-4}$, agree well with the results from the 1C fit.

Since the K_L detection efficiency is low and difficult to determine, K_L detection is not required in the $\gamma K^+K^-K^0_SK^0_L$ channel. Candidates are instead selected by 1C kinematic fits to the hypothesis $J/\psi \to \gamma K^+K^-\pi^+\pi^-(K^0_L)_{miss}$, identifying kaons and pions by TOF and dE/dx. If several kaon- or pion-pair combinations exist, we choose that which best matches a ϕ or a K^0_S. All isolated showers are considered as candidates for the radiative photon. Due to the poor photon-energy resolution, the χ^2 of the 1C fit does not alone provide a sufficient background rejection. The radiative photon is chosen to be that photon for which the quantity

$$\chi^2 + ((m_{K^+K^-} - m_\phi)/\sigma_{K^+K^-})^2 + ((m_{K^0_SK^0_L} - m_\phi)/\sigma_{K^0_SK^0_L})^2$$

is minimal. In order to improve the $K^0_SK^0_L$ mass resolution, a 2C kinematic fit is performed by adding the K^0_S constraint. Candidates are retained if the 2C fit probability is greater than 1%, the event contains either two well-identified kaons or one well-identified kaon and two well-identified pions, and less than four isolated photons are present.

Figure 1b shows the scatter plot of $m_{K^+K^-}$ versus $m_{K^0_SK^0_L}$. A $\phi\phi$ enhancement is again visible. The $\phi\phi$ signal events are selected as above, using the measured resolutions of $\sigma_{K^+K^-} = 3.5$ MeV/c^2 and $\sigma_{K^0_SK^0_L} = 5.6$ MeV/c^2. The resulting $\phi\phi$ invariant mass spectrum contains a total of 119 events (see Figure 2b). The $\phi\phi$ mass resolution varies from 13 MeV/c^2 at 2.2 GeV/c^2 to 30 MeV/c^2 at the η_c. In this case, the background contribution, estimated as above, originates from modes such as $\gamma\phi K^+K^-$, ϕK^+K^-, and $\phi K^+K^-\pi^0$, with $\phi \to K^0_SK^0_L$, and from events containing two kaons, two pions and photons. The background (18%) is again uniform. The hadronic background $J/\psi \to \phi K^0_SK^0_S$ with $K^0_S \to \pi^0\pi^0$ and $\phi \to K^+K^-$ contributes at most one event in the region above 2.8 GeV/c^2.

Figure 2d, showing $m_{\phi\phi}$ in the $\gamma K^+K^-K^0_SK^0_L$ mode after efficiency correction, confirms the $\gamma K^+K^-K^+K^-$ result. The spectrum is fit with the same function used above. In order to obtain stable fits, it was necessary to fix the width of the low-mass Breit-Wigner to the value obtained in the $\gamma K^+K^-K^+K^-$ mode. The mass and product branching ratio for the low mass state are $M = 2214 \pm 20 \pm 15$ MeV/c^2 and $B(J/\psi \rightarrow \gamma X) \cdot B(X \rightarrow \phi\phi) = (2.7 \pm 0.6 \pm 0.6) \times 10^{-4}$. The results, summarized in Table I, confirm those in $\gamma K^+K^-K^+K^-$.

The distributions of the angle between the ϕ decay plane in the $\phi\phi$ rest frame,χ, and the polar angle of the K^+ (or K^0_S) in its ϕ rest frame, θ_K, provide a spin-parity analyzer of states decaying into two vector mesons.[15] Including a background term a, the angular distributions are given by:

$$W(\chi) \propto a + (1-a) \cdot [1 + \beta \cos 2\chi] \quad \text{and}$$

$$W(\cos\theta_K) \propto a + (1-a) \cdot [1 + \frac{\zeta}{2}(3\cos^2\theta_K - 1)]$$

Both β and ζ are functions of the helicity amplitudes characterizing the spin-parity of the intermediate state decaying into $\phi\phi$. Thus a measurement of β determines the parity, since $0 \leq P\beta \leq 1$. For a pseudoscalar, $\beta = -1$ and $\zeta = -1$.

Figures 3a,b show the χ and $\cos\theta_K$ distributions between threshold and 2.40 GeV/c^2 after efficiency correction for both modes combined. While the efficiencies in χ and $\cos\theta_K$ for both pairs $K^\pm K^\mp_{miss}$ and $K^0_SK^0_L$ are uniform, the $\cos\theta_K$ efficiency for the other K^+K^- pair drops near $|\cos\theta_K| = 1$ by 20%. The observed χ distributions peak at large angles, indicating $J^P = (even)^-$. The $\cos\theta_K$ distributions exhibit a strong $\sin^2\theta_K$ dependence, identifying the low-mass structure clearly as a pseudoscalar. A fit, using $W(\chi)$ and $W(\cos\theta_K)$ with $a = 0.11$ yields $\beta = -0.85 \pm 0.11$ and $\zeta = -0.85 \pm 0.13$. To check the reliability of this technique, the χ and $\cos\theta_K$ distributions are examined in the η_c region ($2.90 \leq m_{\phi\phi} \leq 3.05$ GeV/c^2). The resulting distributions are characteristic of a pseudoscalar (see Figures 3c,d). A fit with $a = 0.1$ yields $\beta = -1.0 \pm 0.2$ and $\zeta = -0.70 \pm 0.19$. The parameter β measured in 100 MeV/c^2 mass intervals, is shown in Figure 4. The pseudoscalar component dominates below 2.4 GeV/c^2 and at the η_c.

In order to set a limit on $\xi(2230)$ and $g_T^{16)}$ production in $J/\psi \to \gamma\phi\phi$, a maximum likelihood fit is performed using $W(\chi)$. Assuming that, in addition to a pseudoscalar, partial waves with positive parity are present, the fraction of the $P = +1$ components is given by $f = (1-a)\cdot(1+\beta)/(1+\beta_p)$, where β_p is the average amplitude for the $P = +1$ components and β is the limit determined by integrating the log likelihood over the 90% confidence level interval. Due to unknown phases and relative fractions for the three g_T states, a determination of β_p is not possible. We therefore assume $\beta_p = 0$, which yields the most conservative limit. The resulting upper limits for g_T and $\xi(2230)$ production presented in Table II are obtained by multiplying the observed number of events by f and normalizing the result to the total number of produced J/ψ events after correcting for the detection efficiencies and ϕ decay branching ratios. The limit is a factor of eight higher than a model-dependent prediction for g_T production in radiative J/ψ decays. [17]

In summary, we have observed a pseudoscalar state about 0.15 GeV/c^2 above $\phi\phi$ threshold in the radiative decay $J/\psi \to \gamma\phi\phi$ in two decay channels. This state may correspond to the 200 MeV/c^2 wide pseudoscalar state, $\eta(2100)$, seen in $J/\psi \to \gamma\rho\rho$ at 2.138 GeV/c^2.[11] Additional pseudoscalars have also been seen in $J/\psi \to \gamma\rho\rho$ and $J/\psi \to \gamma\omega\omega$. The nature of these pseudoscalars is not presently understood. Possibilities include the second and third radial excitations of the pseudoscalar mesons[18] as well as $q\bar{q}g$ hybrids[19] or $qq\bar{q}\bar{q}$ states[20].

We gratefully acknowledge the dedicated efforts of the SPEAR staff. One of us (G.E.) wishes to thank the Alexander von Humboldt Foundation for support. This work was supported in part by the U.S. Department of Energy, Contracts DE-AC03-76SF00515, DE-AC02-76ER01195, DE-AC03-81ER40050 and DE-AM03-76SF00034 and by the National Science Foundation.

References

1. See references given in G. Eigen, Spectroscopy of light and heavy Quarks, Ed. by U. Gastaldi, R. Klapisch and F. Close, Ettore Majorana Series Vol. 37.
2. A. Etkin *et al.*, Phys. Lett. **B201**, 568 (1988) and references therein; C. Daum *et al.*, Phys. Lett. **B104**, 246 (1981); T.F. Davenport *et al.*, Phys. Rev. **D33**, 2519 (1986); P.S.L. Booth *et al.*, Nucl. Phys. **B273**, 677 (1986).
3. S.J. Lindenbaum & R.S. Longacre, Phys. Lett. **B165**, 202 (1985).
4. D. Bisello *et al.*, Phys. Lett. **B179**, 294 (1986).
5. D.L. Burke *et al.*, Phys. Rev. Lett. **49**, 632 (1982); R.M. Baltrusaitis *et al.*, Phys. Rev. **D33**, 1222 (1986); M. Bisello *et al.*, Phys. Rev. **D39**, 701 (1989). R.M. Baltrusaitis *et al.*, Phys. Rev. Lett. **55**, 1723 (1985).
6. An earlier analysis of these final states is given in B. Tripsas, Ph.D. thesis, University of Illinois at Urbana Champaign, 1988 (unpublished).
7. D. Bernstein *et al.*, Nucl. Instr. Meth. **226**, 302 (1984).
8. Isolated photons are showers of at least 40 MeV, which begin within the first seven radiation lengths of the sampling calorimeter (9 layers), contain at least two layers and lie outside a 20° cone around each charged track.
9. We use TOF for particle identification; dE/dx is used only if TOF is not available. A kaon well-identified by TOF is any track with a measured TOF lying within 4 s.d. of the K prediction and favoring a K hypothesis over the π hypothesis. A kaon well-identified by dE/dx is any track which favors a K hypothesis within 4 s.d. and is separated from the π hypothesis by more than 4 s.d. A pion candidate is any track with a measured TOF (dE/dx) being consistent with a π hypothesis within 5 (4) s.d.
10. J.D. Jackson, Nuov. Cim. **34**, 1644 (1964). Bose-Einstein correlations are negligible; the ϕ is narrow and K^+K^- pair selection is largely unambiguous.

11. We have tested the hypothesis that the low-mass $\phi\phi$ state is connected to the $\eta(2100)$ observed in $\gamma\rho\rho$. Were we to assume the $\eta(2100)$ decays dominantly to channels other than $\phi\phi$, the total width would be independent of the $\phi\phi$ kinematics. Then the $\gamma K^+K^-K^+K^-$ mass and width would be $M = 2196 \pm 20$ MeV/c^2 and $\Gamma = 110 \pm 50$ MeV/c^2. Similar results are found for the other channel.

12. N. Törnqvist, Act. Phys. Pol. **B16**, 503 (1984) and private communication.

13. M. Aguilar-Benitez *et al.*, Phys. Lett. **170B**, 1 (1986).

14. R.M. Baltrusaitis *et al.*, Phys. Rev. Lett. **52**, 2126 (1984).

15. T. L. Trueman, Phys. Rev. **D18**, 3423 (1978). N.P. Chang & C.A. Nelson, Phys. Rev. **D20**, 2923 (1979).

16. The g_T's correspond to $f_2(2010)$, $f_2(2050)$, and $f_2(2340)$ in the Particle Data Group classification.

17. R. Sinha, S. Okubo & S.F. Tuan, Phys. Rev. **D35**,952 (1987). In $J/\psi \rightarrow \gamma\rho\rho$ this prediction was found to be inconsistent with a limit determined by DM2.[5)]

18. D.P. Stanley & D. Robson Phys. Rev. **D21**, 3180 (1980); S. Godfrey & N. Isgur, Phys. Rev. **D32**, 189 (1985).

19. M. Chanowitz & S. Sharpe, Nucl. Phys. **B222**, 391 (1981).

20. B.A. Li, Proc. of Tau/Charm Workshop, SLAC-PUB-5007, 816 (1989) and private communication.

Table I. Fit Results for the $\phi\phi$ Mass Spectra from the $\gamma K^+K^-K^+K^-$ and $\gamma K^+K^-K^0_SK^0_L$ final states			
final state	Mass [MeV]	Width [MeV]	$B(J/\psi \to \gamma X) \cdot B(X \to \phi\phi)^\dagger$
$\gamma K^+K^-K^+K^-$	$2230 \pm 25 \pm 15$	$150\,^{+300}_{-60} \pm 60$	$(3.3 \pm 0.8 \pm 0.5) \times 10^{-4}$
$\gamma K^+K^-K^0_SK^0_L$	$2214 \pm 20 \pm 15$	150 fixed	$(2.7 \pm 0.6 \pm 0.6) \times 10^{-4}$
$\gamma K^+K^-K^+K^-$	$2981 \pm 8 \pm 3$	10.3 fixed	$(0.93 \pm 0.20 \pm 0.16) \times 10^{-4}$
$\gamma K^+K^-K^0_SK^0_L$	$2956 \pm 12 \pm 12$	10.3 fixed	$(0.85 \pm 0.27 \pm 0.18) \times 10^{-4}$

† The systematic errors in the branching ratios include the following contributions which are added in quadrature: uncertainties in the luminosity measurement (8.5%), uncertainties from the event selection, background subtraction and efficiency determination (13% for $\gamma K^+K^-K^+K^-$ and 18% for $\gamma K^+K^-K^0_SK^0_L$), and uncertainties in the fit (6%).

Table II. Upper limits for g_T and $\xi(2230)$ production in $J/\psi \to \gamma\phi\phi$					
Mass region [GeV]	Number of events	β_p	$\epsilon_{\gamma K^+K^-K^+K^-}$	$\epsilon_{\gamma K^+K^-K^0_SK^0_L}$	$B(J/\psi \to \gamma X) \cdot B(X \to \phi\phi)$
g_T (2.04-2.40)	122	0.29	0.12	0.14	$< 1.16 \times 10^{-4}$ at 90% CL.
$\xi(2230)$ (2.20-2.26)	32	0.39	0.12	0.15	$< 0.38 \times 10^{-4}$ at 90% CL.

Figure Caption

Figure 1. Scatter plots for $J/\psi \to \gamma 4K$: a) $m_{K^+K^-}$ versus $m_{K^\pm K^\mp_{miss}}$; b) $m_{K^+K^-}$ versus $m_{K^0_S K^0_L}$. Events in the shaded regions are used for background estimated.

Figure 2. The observed $\phi\phi$ invariant mass spectra from (a) $J/\psi \to \gamma K^+K^-K^+K^-$ and (b) $J/\psi \to \gamma K^+K^-K^0_S K^0_L$; c,d) the corresponding $\phi\phi$ invariant mass spectra after efficiency correction. Shaded histograms show background estimates; dashed curves show detection efficiencies denoted by ϵ; solid curves show fits described in the text.

Figure 3. Angular Distributions for $J/\psi \to \gamma\phi\phi$ after efficiency correction for both modes combined: a,b) The χ and $\cos\theta_K$ distributions for the low-mass state (2.05-2.39 GeV/c^2), c,d) The χ and $\cos\theta_K$ distributions for the η_c (2.92-3.04 GeV/c^2). The solid curves show fits described in the text.

Figure 4. The amplitude β as a function of $m_{\phi\phi}$.

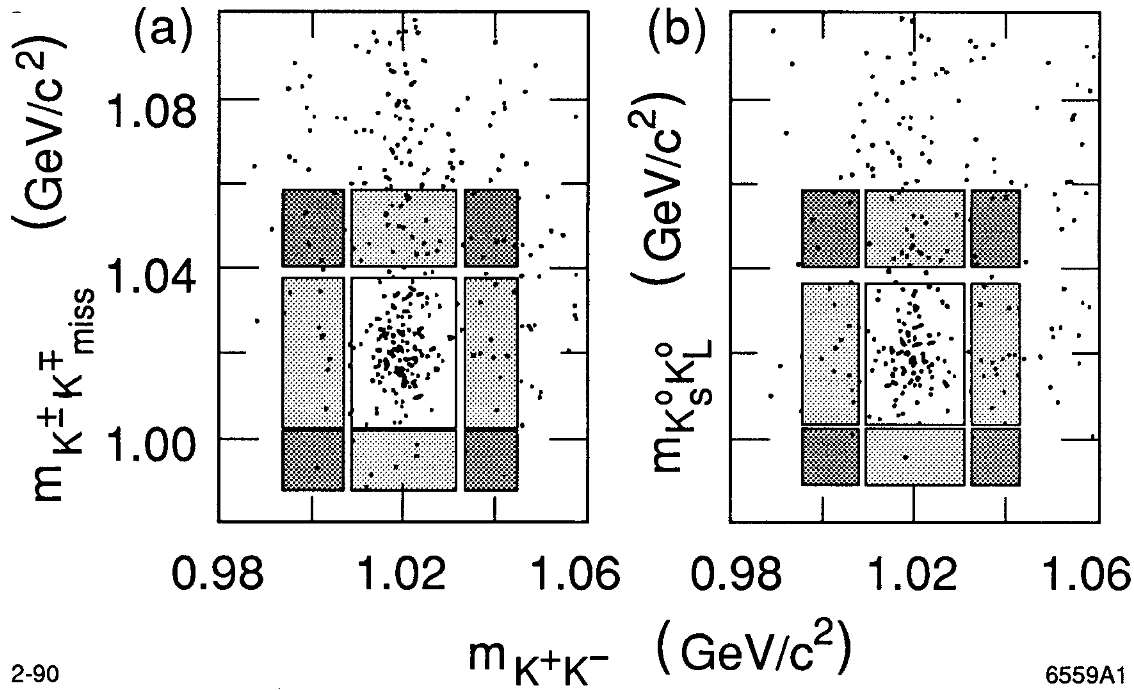

(a)
(b)
1.08
1.04
1.00
0.98
1.02
1.06
$m_{K^\pm K^\mp_{miss}}$ (GeV/c^2)
$m_{K^o_s K^o_L}$ (GeV/c^2)
$m_{K^+K^-}$ (GeV/c^2)
2-90
6559A1

Fig. 1

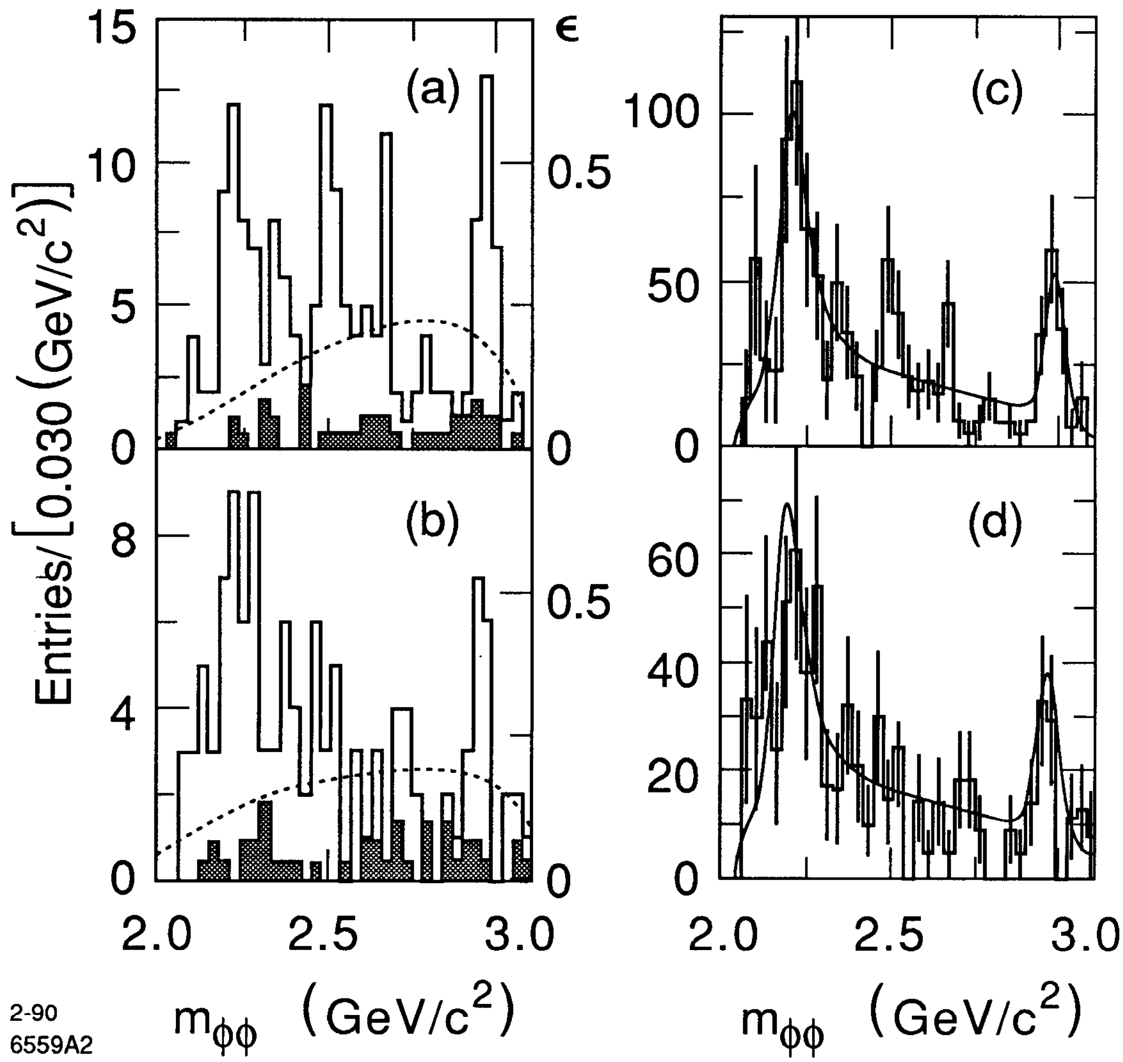
15
10
5
0
8
4
0
ϵ
0.5
0
0.5
0
(a)
(b)
(c)
(d)
100
50
0
60
40
20
0
Entries/[0.030 (GeV/c²)]
2.0
2.5
3.0
2.0
2.5
3.0
m_ϕϕ (GeV/c²)
m_ϕϕ (GeV/c²)
2-90
6559A2

Fig. 2

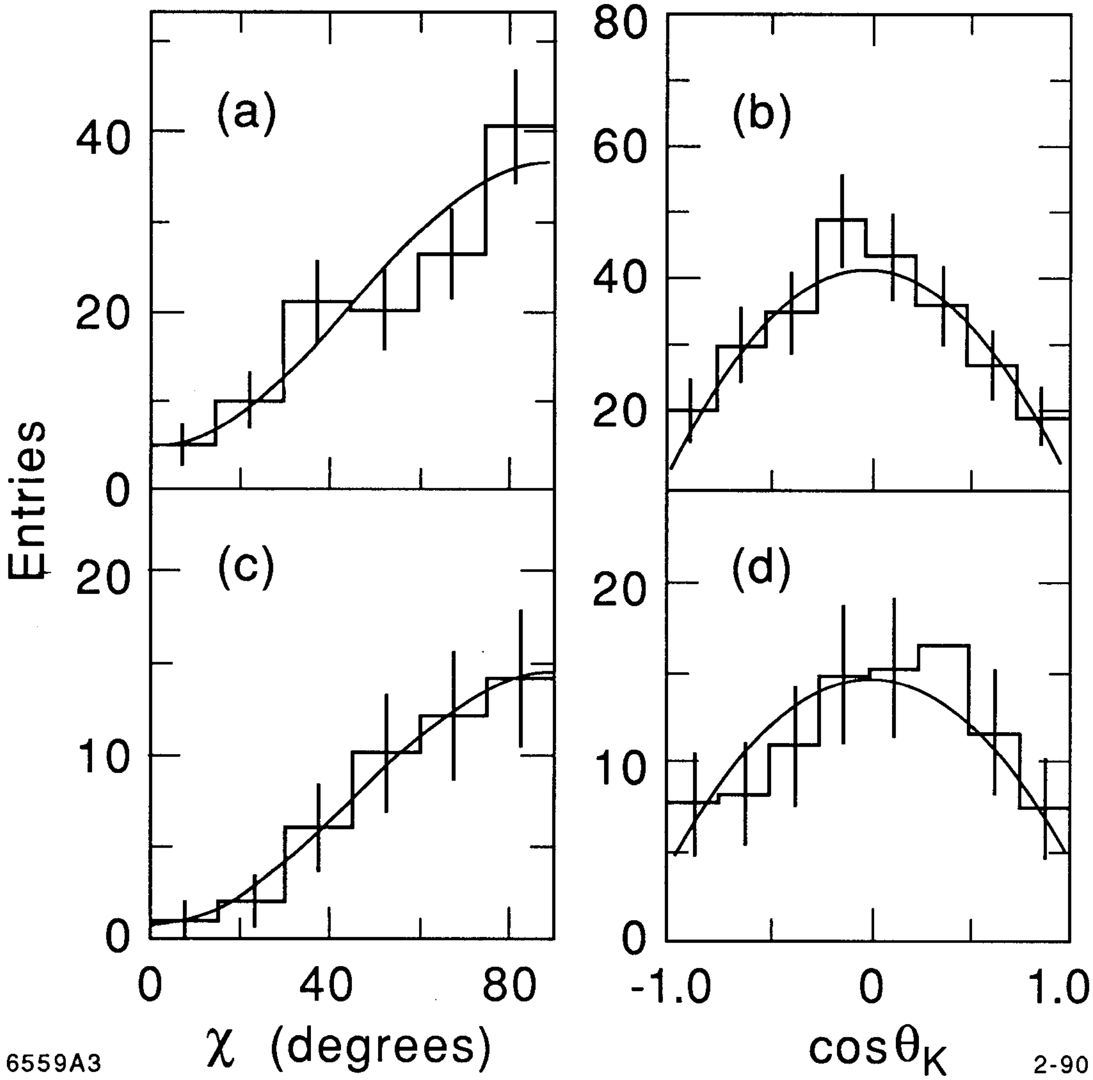

Fig. 3

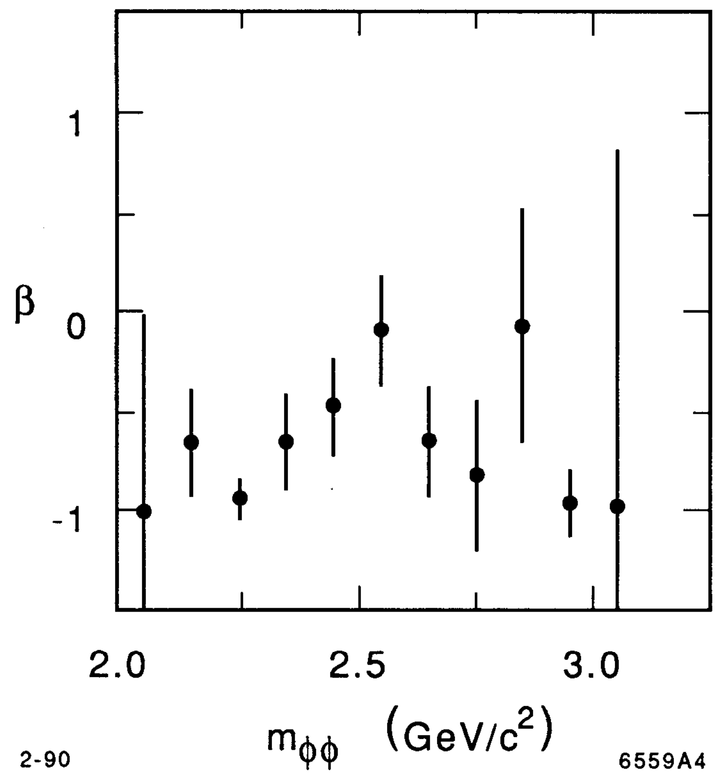

Fig. 4